

Fault-adaptive traffic demand estimation using network flow dynamics

Yirolanda Englezou, Member, IEEE, Stelios Timotheou, Senior Member IEEE
and Christos G. Panayiotou, Senior Member, IEEE

Abstract—Estimating traffic demand, or origin-destination (OD) matrices, is crucial for transport studies and smart city development. The main objective is to calculate an OD matrix based on available sources (e.g. link traffic counts obtained from traffic sensors) to accurately reproduce field data. A significant complication when using information obtained from traffic sensors, is that such sensors are subject to considerable disruptions impacting data quality and reliability. Despite the extensive study of efficient OD estimation, there is a considerable gap in detecting faulty measurements and identifying faulty sensors within the estimation procedure. This work presents a novel methodology for OD matrix estimation in the presence of faulty measurements. The path-based cell transmission model (CTM) is employed to capture traffic network dynamics within a specified time window, linking link densities with per-path densities and path demand. For the purposes of this work, traffic networks that operate under free-flow conditions are considered and the problem is formulated in an optimisation framework with two distinct variations: (i) no explicit formulation of potential faulty sensors and (ii) explicit modelling of potential faulty sensors. Following, a fault-adaptive algorithm is constructed that identifies, isolates and corrects faults to achieve robust demand estimation. The methodology is tested on two realistic literature networks and shows great potential in terms of OD matrix estimation in the presence of faulty measurements. Simulation results underpin the advantage of the proposed approach in terms of performance in estimating quantities of interest as well as identifying the faulty sensors and their fault characteristics.

I. INTRODUCTION

Motivation. Accurately estimating the origin-destination (OD) matrix for a given network is essential in the field of transportation, as it allows practitioners to improve network planning and management, while it provides researchers with data to validate novel monitoring and control methods. These matrices are typically used as inputs to network equilibrium models, that are important tools for traffic modelling and planning purposes. The OD matrix cannot be directly observed, necessitating the development and testing

This work is supported by the European Union (i. ERC, URANUS, No. 101088124 and, ii. Horizon 2020 Teaming, KIOS CoE, No. 739551), and the Government of the Republic of Cyprus through the Deputy Ministry of Research, Innovation, and Digital Strategy. Views and opinions expressed are however those of the author(s) only and do not necessarily reflect those of the European Union or the European Research Council Executive Agency. Neither the European Union nor the granting authority can be held responsible for them.

Y. Englezou, S. Timotheou and C.G. Panayiotou are with the KIOS Research and Innovation Center of Excellence, and the Department of Electrical and Computer Engineering, University of Cyprus. {englezou.yirolanda, timotheou.stelios, christosp}@ucy.ac.cy

of various approaches, to efficiently address the OD matrix estimation challenge over the years.

Related work. The estimation of OD matrices has been widely explored in the literature, often using link counts (i.e., the number of vehicles passing through specific links) and a variety of proposed models. This process aims to find a solution within a defined feasible space, while adhering to traffic flow constraints, such as maintaining non-negative OD values. Although traditional methods like roadside interviews and travel surveys provide useful data, they are often expensive and may lack sufficient trip coverage for many elements of the matrix. To overcome these challenges, traffic count-based OD matrix estimation has been developed as an alternative. The main objective is to compute an OD matrix from available traffic counts, ensuring the best possible match to observed field data. For a thorough overview of OD matrix estimation methodologies, refer to [1], [2].

Two distinct formulations are commonly considered for OD matrix estimation, the *static*, or *time-independent* and *dynamic* or *time-dependent* problems. In the time-independent OD matrix estimation, traffic inflows are treated as time-independent, formulating the estimation as a steady-state scenario over a fixed period T . In this context, the average OD demand is computed over a specified time window T , based on a single set of link counts, without considering variations in traffic flows over time (e.g., [3], [4], [5], [6], [7], among others). In contrast, dynamic OD estimation is tailored for short-term traffic operation applications, such as route guidance and dynamic traffic assignment. This dynamic problem involves time-dependent traffic data collected in small intervals, typically 10-15 minutes, aiming to estimate time-varying OD matrices (e.g., [8], [9], [10], [11], [12], and many others). The OD matrix estimation problem is highly challenging due to its underdetermined nature, large-scale complexity, computational intensity, and nonlinear relationship between traffic counts and OD demands [13], [14]. To address this complexity, various assumptions and considerations are often introduced concerning available data sources, models describing the relationship between OD demands and traffic data, and the corresponding solution approaches. These assumptions encompass the nature of available observations, traffic conditions, and behaviours, all of which play a critical role in formulating the mathematical relationship between observations and OD demands.

Related work - Models. Various models, including microscopic, mesoscopic, and macroscopic, have been proposed over the years to address the OD matrix estimation problem. These include simulation models, statistical methods, and

generalized least squares models. Path flow estimation (PFE) models have also been proposed to estimate OD matrices by inferring optimal path flows through linear programming, aiming to match user-equilibrium flow patterns, reproduce link traffic counts and reproduce a target OD matrix as closely as possible [15]. Early PFE methods required enumerating paths or using column generation, which was computationally inefficient, while later approaches decoupled the linear model, using k-shortest path algorithms to find equilibrium paths to address this issue [16]. However, PFE models are inefficient when the target OD matrix contains significant errors. Solutions have been proposed, including generalized least squares (GLS) [17] and heuristic methods [18], which still rely on a target OD matrix. Recent models have incorporated multimodal transportation and macroscopic techniques using link densities instead of flows [19], [20], though these approaches face challenges due to non-convexity and non-differentiability [21]. A novel path-based methodology was recently introduced, which uses fine-grained measurements and a macroscopic model to associate link counts with path demands, yielding accurate results in both free-flow and congested conditions [22].

Related work - Solution Approaches. Various solution approaches have been explored to address the OD estimation problem, incorporating a combination of available data and models. A common approach involves assuming a known routing matrix and iteratively alternating between OD estimation and traffic assignment until convergence is reached. Alternatively, some approaches are based on bi-level optimization problems [23]. Several researchers, including [24], [14], [11], and [25], have also successfully applied Kalman filtering techniques to dynamic OD matrix estimation problems. Recently, deep learning approaches that construct layered computational graphs have gained popularity [26], [27]. However, despite their potential, these methods often face significant computational challenges, limiting their feasibility for large-scale problems. Additionally, due to the non-convexity of these problems, they tend to produce locally optimal solutions [26]. Another innovative method uses convolutional neural networks to estimate time-dependent OD flows, as shown in [28]. Many of these approaches rely on a prior, or target, OD matrix derived from historical data as an input for solving the OD estimation problem. A major drawback is that poor-quality samples used to generate the prior matrix can result in significant OD estimation errors [29].

Related work - Sensor Data. In this work, we adopt a model-based approach utilizing available link data gathered from static traffic sensors, e.g. loop detectors. Such sensors are used to collect measurements of the flow at observed links (e.g. links that are equipped with loop detectors), as well as to provide information for inference at unobserved links. However, a significant challenge when relying on data from traffic sensors, is that such sensors are susceptible to significant disruptions due to system errors, diminishing the quality and reliability of the information they provide [30]. The potential issues associated with traffic sensors include bias, drifting, or complete failure, all of which compromise

the accuracy and dependability of the sensor measurements, yielding incorrect information. Studies on sensor network measurements have revealed that approximately 20%-30% of traffic sensors may experience some form of failure [31], [32], [33]. Sensor failures have to be explicitly accounted in the OD matrix estimation process to ensure efficiency and reliability. Failure to address sensor faults explicitly can lead to erroneous data, potentially resulting in suboptimal traffic management strategies and impacting travel decisions of network users [34].

Most studies on faulty traffic sensors concentrate on traffic state estimation, typically addressing three key aspects: fault detection, fault correction, and state estimation. Effective state estimation in the presence of sensor faults depends heavily on prompt and accurate fault detection and isolation, a process known as fault-tolerant estimation [35], [36]. For detecting faults, a common approach involves using probabilistic measures (such as the likelihood of counting a certain number of vehicles) alongside a pre-defined range (based on physical limits or empirical data) to flag measurements as faulty when they fall outside the expected range [32], [37], [38]. However, a limitation of these methods is that obtaining reliable results often requires considering a long time horizon (up to one day), making real-time fault detection difficult. Other methods have been proposed that detect faulty measurements by comparing them to historical data or predicted values [39], [40], but these approaches can struggle to identify faults in the face of changing traffic patterns. Some research on faulty traffic sensors also focuses on sensor placement for flow observability and estimation, aiming to either maximize information gain from origin-destination (OD) routes, or minimize errors in freeway performance monitoring when sensors fail [41], [42]. A data-driven approach for predicting traffic flow at locations with faulty sensors was proposed, using a polynomial function of current traffic flow to approximate future flow [43]. While this method showed good predictive accuracy, it required a substantial amount of historical data for training. To overcome the challenges posed by traditional methods that often treat state estimation and fault detection/correction as separate steps, a real-time moving horizon estimation approach was introduced [44]. This method simultaneously achieves robust traffic state estimation and fault identification [45], demonstrating its effectiveness through the use of the cell transmission model (CTM) to account for network-wide traffic dynamics and transitions between links. To the best of our knowledge, the combined task of simultaneously identifying sensor faults and estimating OD matrices has not yet been explored in the literature.

When a sensor is faulty, the measurements are subject to abrupt changes, also known as change points in time series data, within the total time horizon under study. Change-point detection has been extensively studied in the literature [46]. This problem has been thoroughly examined within the statistical framework over the past few decades, where various approaches have been examined. A common statistical approach to change-point detection involves considering probability distributions that generate data in both past and

present intervals. The target time point is then identified as a change-point if there is a significant difference between the two distributions [47]. Bayesian approaches that predict the probability distributions of the upcoming interval using data observed since the last identified candidate change-point [48], have also been examined. Further, many machine learning algorithms have been designed, enhanced, and adapted for change-point detection. Kernel-based methods map observations onto a higher-dimensional feature space and detect change-points by comparing the homogeneity of each subsequence [49]. Clustering methods, have also been employed, where a known or unknown number of clusters is considered, where if a data point at time t belongs to a different cluster than the data point at time $t + 1$, then a change point occurs between the two observations [50]. In the context of supervised approaches for change point detection, machine learning algorithms are trained as either binary or multi-class classifiers [51].

In this work, we opt to use a recently introduced algorithm grounded in the Bayesian framework. Bayesian inference does not typically prioritise one model as the ‘correct’ model but rather considers the value and applicability of all possible models. In the context of Bayesian model averaging [52], each model is assigned a probability of being the true model, based on the data. This probability acts as an informative weight, enabling the combination of all models into a weighted average, which helps to address issues like model misspecification and uncertainty across different models. The Bayesian Estimator of Abrupt change, Seasonality, and Trend (BEAST) algorithm is a parametric regression approach that avoids the need for threshold testing or criterion optimization. Instead, it fits a global model to the entire time series in one step, identifying change points, trends, and seasonality simultaneously. The BEAST algorithm is publicly available from GitHub [53].

Contributions. We formulate the OD matrix estimation problem under the assumption that sensor measurements may be faulty. We study networks that operate under free-flow conditions and adopt a model-based approach, i.e. the path-based CTM is used, to estimate time-independent¹ OD matrices in a pre-specified time period T utilizing available link data gathered from static traffic sensors, while identifying and correcting faulty measurements. The use of the path-based CTM allows us to take into account traffic counts in smaller intervals (e.g. every 10-15 seconds) in the pre-specified time period. Our work attempts to fill a gap in the literature by making the following main contributions:

- We employ a path-based CTM for estimating OD matrices in scenarios with faulty measurements within networks operating under free-flow conditions. This results in a state space model where link densities (measurements) are linked to per-path densities (state vector) and the path demand pattern. This formulation facilitates the creation of a convex optimisation prob-

lem with the objective of minimising the discrepancy between the model and the actual measurements.

- We propose a novel OD matrix estimation methodology that explicitly models potential faulty sensors. Our approach presents a robust estimation strategy for the identification and isolation of faulty sensors along with estimation of their faulty magnitudes.
- We develop a fault-adaptive algorithm that simultaneously accomplishes two key objectives: (i) precise OD matrix estimation and (ii) identification and correction of the faulty sensor measurements. This approach allows the efficient estimation of the OD matrix of the network under study even when the deployed sensors are subject to failures.

The proposed approach is tested on literature networks that operate under the free-flow regime when there are available (i) full measurements (loop detectors on all road segments in the network) and (ii) partial measurements (loop detectors on a subset of road segments).

Our main contribution is the effective estimation of OD matrices in the presence of faulty measurements, a challenge that has not yet been explored in the literature. Towards this direction, two additional novel aspects that emerge are (i) the extension of our path-based OD matrix estimation scheme, recently introduced in [22]², to account for measurement and model noise, and (ii) the detection of faults, the identification of faulty sensors, and the correction of faulty measurements. In addition, important features of this work arise from the formulation of the problem using fine-grained measurements as follows: (i) no prior or target OD matrices are needed to implement the approach, outlasting the bias and dependency on such matrices³, (ii) no route choice models or split ratios are needed, (iii) no user equilibrium conditions are required for high-quality estimation, (iv) no historical data are required for accurate estimations, and (v) even low partial coverage of the network is sufficient to provide high-quality OD matrix estimations.

Paper structure. The remainder of the paper is organised as follows. In the next section we set up the network notation. In Section III we introduce the path-based CTM, i.e. the model used to capture traffic dynamics. In Section IV-A the optimisation problem for OD matrix estimation is introduced and the state space model is formulated in the context of the path-based CTM. Section V shows the optimisation solution approach for OD estimation under two distinct variations: (i) no explicit formulation of potential faulty sensors and (ii) explicit modelling of potential faulty sensors. Section VI demonstrates the simulation results obtained by the proposed approach. Last, in Section VIII the main performance results are summarised and future research directions are presented.

²In [22] we introduced a general state-space model that utilizes the signalized path-based CTM to represent traffic dynamics and addressed the OD matrix estimation problem in a noise-free environment and no consideration of faults.

³Prior or target OD matrices often require manual interview and survey methods that take several months to be completed, and hence might not be available for most networks.

¹The ‘time-independent’ term aims to reflect that the OD matrix is fixed and does not vary over the considered time horizon in our approach

Notation. In the remainder of this paper we use the following notation. All bold letters indicate vectors (lower case) or matrices (upper case), while calligraphic letters denote sets. If \mathcal{A} is a set we denote as $|\mathcal{A}|$ the cardinality of the specific set. The subset $\mathbb{R}_+ \subset \mathbb{R}$ contains the real numbers that are equal or greater than zero. The superscripts $(\cdot)^T$ and $(\cdot)^{-1}$, denote the transpose and the matrix inverse respectively. In addition $\|\mathbf{x}\|_{[\mathbf{A}]}^2 = \mathbf{x}^T \mathbf{A} \mathbf{x}$ denotes the Euclidean weighted norm and $\|\mathbf{x}\|^2 = \mathbf{x}^T \mathbf{x}$ the Euclidean norm of a vector \mathbf{x} . A block diagonal matrix is defined as $\text{blkdiag}(\mathbf{A}_1, \dots, \mathbf{A}_n)$, which is a square diagonal matrix in which the diagonal elements are the square matrices \mathbf{A}_i and the off-diagonal elements are zero. The (i, j) th element of a matrix \mathbf{A} is denoted as $\mathbf{A}_{[i,j]}$. Further, $\mathbf{I}_{n \times n}$ is the $n \times n$ identity matrix and $\mathbf{0}_{n \times n}$ denotes a $n \times n$ matrix that all its elements are zero. Furthermore, $x \sim \mathcal{N}(\mu, \sigma^2)$ indicates that x is a random variable drawn from the normal distribution with mean μ and variance σ^2 .

II. NETWORK NOTATION

Consider a directed graph $\mathcal{G} = (\mathcal{V}, \mathcal{E})$, where \mathcal{V} is the set of V nodes and \mathcal{E} the set of directed road links, each composed of multiple road segments. Let \mathcal{L} denote the set of all road segments⁴. The graph is associated with W OD pairs, where $W \leq V \times (V - 1)$. The set of road segments equipped with fixed-location sensors is denoted by $\mathcal{C} \subseteq \mathcal{L}$, and \mathcal{W} represents the set of OD pairs, with $W = |\mathcal{W}|$. Let $L = |\mathcal{L}|$ be the total number of road segments, and $C = |\mathcal{C}| \leq L$ the number of road segments equipped with static sensors (e.g., loop detectors).

For each OD pair $w \in \mathcal{W}$, the demand is distributed across various paths in the graph. Let $\mathcal{P} = \{p_1, p_2, \dots, p_Q\}$ represent the set of all candidate paths⁵ in \mathcal{G} , where $Q = |\mathcal{P}|$ is the total number of paths. Each road segment $i \in \mathcal{L}$ is associated with one or more paths from \mathcal{P} , denoted by \mathcal{P}_i , which is the set of candidate paths passing through road segment i , and $P_i = |\mathcal{P}_i|$ is the number of paths associated with segment i . The total number of path-segment associations across all road segments is given by $M = \sum_{i \in \mathcal{L}} P_i$. Finally, for each OD pair $w \in \mathcal{W}$, there exists a set of candidate paths \mathcal{S}_w representing possible routes for the demand of that OD pair, such that the set of all paths \mathcal{P} is the union of the paths for all OD pairs, i.e., $\mathcal{P} = \cup_{w \in \mathcal{W}} \mathcal{S}_w$.

III. TRAFFIC NETWORK MODEL

The cell transmission model (CTM) is a widely used macroscopic traffic flow model [55], [56], commonly applied in traffic control, network modeling, and the analysis of road network stability. Each cell i is defined by several key parameters: the free-flow speed, v_i^f (km/h), the backward wave speed, v_i^b (km/h), the maximum flow rate, φ_i^{max}

⁴A road segment is defined as a distinct and measurable section of a link between two defined points, typically characterized by attributes such as length and associated features. For instance, a 1 km road link may be divided into four 250 m road segments.

⁵Candidate paths can be generated using a variant of the k-shortest paths algorithm for transportation networks, which identifies the top shortest paths that significantly differ in the road segments they traverse [54].

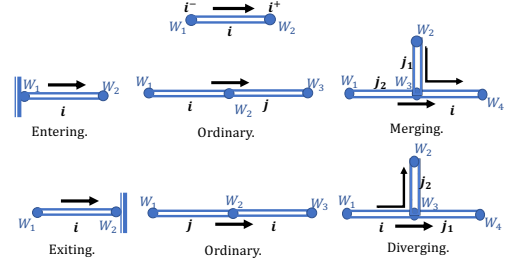


Fig. 1: Upstream and downstream boundary connections.

(veh/h), the maximum density, ρ_i^{max} (veh/km), and the cell length, l_i .

In the discrete-time version of the model, a sampling time T_s is selected, which must satisfy the Courant-Friedrichs-Lewy (CFL) condition for stability [57]. This condition ensures that a vehicle cannot both enter and exit the same cell during a single time-step, requiring the inequality $v_i^f T_s \leq l_i$ to hold for all cells in the network. Boundary connections occur where cells merge or diverge. The set of upstream neighbors is denoted by \mathcal{N}^- , and the downstream neighbors by \mathcal{N}^+ . If traffic flows from cell i into cell j , then $i \in \mathcal{N}_j^-$ and $j \in \mathcal{N}_i^+$. As described in [7], the inflow, $\bar{\varphi}_i^{in}(t)$, and outflow, $\bar{\varphi}_i^{out}(t)$, of each cell i are determined by the boundary connections between adjacent cells. The upstream connection for each cell, i^- , can be classified as ordinary (\mathcal{O}), entering (\mathcal{E}), or merging (\mathcal{M}), while the downstream connection, i^+ , may be ordinary (\mathcal{O}), diverging (\mathcal{D}), or exiting (\mathcal{G}) (refer to Figure 1).

The vehicle density in cell i , denoted by $\bar{\rho}_i(t)$, is influenced by the inflow and outflow of vehicles, following the demand and supply principle [58]. The demand, expressed as $D_i(t) = \min\{v_i^f \bar{\rho}_i(t), \varphi_i^{max}\}$, represents the number of vehicles attempting to exit cell i at time t . The supply, given by $S_i(t) = \min\{\varphi_i^{max}, v_i^b [\rho_i^{max} - \bar{\rho}_i(t)]\}$, indicates the number of vehicles that cell i can accommodate at time t , based on its storage capacity. The evolution of the traffic density, $\bar{\rho}_i(\cdot)$, in cell i is described by the equation:

$$\bar{\rho}_i(t+1) = \bar{\rho}_i(t) + \frac{T_s}{l_i} [\bar{\varphi}_i^{in}(t) - h_i(t) \bar{\varphi}_i^{out}(t)]. \quad (1)$$

Above, $h_i(t)$ represents the traffic signal controlling the outflow of vehicles from cell $i \in \mathcal{L}$, where $h_i(t) = 1$ during the green phase and $h_i(t) = 0$ during the red phase.

A. Signalised path-based cell transmission model

The path-based CTM [59], [7] builds upon the traditional CTM by enabling tracking of vehicle densities and flows for individual paths, removing the need for strict assumptions about split ratios. This model enhances the efficiency of OD matrix estimation through the assessment of path demands and application of Equation (6). For each path p passing through cell i , the density is updated as follows:

$$\rho_{i,p}(t+1) = \rho_{i,p}(t) + \frac{T_s}{l_i} [\varphi_{i,p}^{in}(t) - h_i(t) \varphi_{i,p}^{out}(t)]. \quad (2)$$

As in the previous section, the per-path inflows and outflows for cell i are determined by its boundary connections. In

networks with free-flow conditions, if i^- belongs to \mathcal{O}, \mathcal{M} , the inflow is calculated as $\varphi_{i,p}^{in}(t) = v_j^f \rho_{j,p}(t)$ for $p \in \mathcal{P}_i \cap \mathcal{P}_j$ and $j \in \mathcal{N}_i^-$, while if i^- is in \mathcal{E} , the inflow is $\varphi_{i,p}^{in}(t) = u_p$, where $u_p(t)$ represents vehicles entering the network at time t . Similarly, for free-flow conditions and i^+ in $\mathcal{O}, \mathcal{D}, \mathcal{G}$, the outflow is $\varphi_{i,p}^{out}(t) = v_i^f \rho_{i,p}(t)$ for $p \in \mathcal{P}_i \cap \mathcal{P}_j$ and $j \in \mathcal{N}_i^+$. Here, \mathcal{P}_i and \mathcal{P}_j denote the sets of paths passing through cells i and j , respectively. Equations (1) and (2) are connected by the fact that the overall density, inflow, and outflow for cell i are the sums of the respective values for all paths associated with that cell:

$$\begin{aligned}\bar{\rho}_i(t) &= \sum_{p \in \mathcal{P}_i} \rho_{i,p}(t) \\ \bar{\varphi}_i^{in}(t) &= \sum_{p \in \mathcal{P}_i} \varphi_{i,p}^{in}(t), \quad \bar{\varphi}_i^{out}(t) = \sum_{p \in \mathcal{P}_i} \varphi_{i,p}^{out}(t).\end{aligned}$$

For further information on the path-based CTM, refer to [7].

IV. PROBLEM STATEMENT

A. OD matrix estimation problem

We focus on networks operating within a free-flow regime throughout the entire observation period T . This period is divided into K time intervals, each of length T_s [hours], with $\mathcal{T}^+ = 1, \dots, K$ and $\mathcal{T} = 0, \dots, K-1$, where $K = T/T_s$. The sampling interval T_s defines both the measurement frequency and the discrete time steps of the traffic model. Under free-flow conditions, the system is mathematically represented by a traffic state evolution model and an observation model of the form

$$\begin{aligned}\mathbf{x}_{t+1} &= \mathbf{A}_t \mathbf{x}_t + \mathbf{B} \mathbf{u} + \boldsymbol{\epsilon}_t, \\ \mathbf{y}_t &= \mathbf{H} \mathbf{x}_t + \boldsymbol{\omega}_t,\end{aligned}\tag{3}$$

where $\mathbf{x}_t \in \mathbb{R}^{(L+M) \times 1}$ denotes the state vector at time t , with \mathbf{x}_0 representing the initial state. The vector $\mathbf{u} \in \mathbb{R}^{Q \times 1}$ encompasses unknown inputs⁶, and $\mathbf{y}_t \in \mathbb{R}^{C \times 1}$ represents noisy observations, assumed to be conditionally independent. The matrix $\mathbf{A}_t \in \mathbb{R}^{(M+L) \times (M+L)}$ defines the state transition⁷, while $\mathbf{H} \in \mathbb{R}^{C \times (M+L)}$ relates the state to the observations. Since \mathbf{H} and \mathbf{B} do not change over time, we do not use subscript t . Errors $\boldsymbol{\epsilon}_t \sim \mathcal{N}(\mathbf{0}, \boldsymbol{\Sigma}_t^\epsilon)$ and $\boldsymbol{\omega}_t \sim \mathcal{N}(\mathbf{0}, \mathbf{Z}_t^\omega)$ are assumed to be Gaussian, with $\boldsymbol{\Sigma}_t^\epsilon \in \mathbb{R}^{(M+L) \times (M+L)}$ and $\mathbf{Z}_t^\omega \in \mathbb{R}^{C \times (M+L)}$ representing the model and measurement error matrices, respectively.

The measurement vector \mathbf{y}_t corresponds to observed traffic variables, such as the traffic density $\bar{\rho}(t)$ on specific road segments at time t , while \mathbf{x}_t represents the unobserved states, such as the density of each candidate path on road segment i at time t , $t \in \mathcal{T}$. The input vector $\mathbf{u} = [u_1, \dots, u_Q]^T$ denotes the path-based demand entering the network at each path $p = 1, \dots, Q$. Rewriting Equations (3) in vector form, yields

$$\begin{aligned}\mathbf{C} \mathbf{X} &= \mathbf{A}_* \mathbf{X} + \mathbf{B}_* \mathbf{u} + \mathbf{b}_* + \boldsymbol{\epsilon}, \\ \mathbf{Y} &= \mathbf{H}_* \mathbf{X} + \boldsymbol{\omega},\end{aligned}\tag{4}$$

⁶Vector \mathbf{u} is considered time-independent, i.e., $\mathbf{u}_t = \mathbf{u}, \forall t$, as the OD demands are assumed static and homogeneous for each path.

⁷Matrix \mathbf{A}_t is time-dependent due to the effect of traffic signals, through the presence of parameter $h_i(t)$ in Equations (1) and (2).

for all $t \in \mathcal{T}$, where $\mathbf{X} = [\mathbf{x}_1^T, \mathbf{x}_2^T, \dots, \mathbf{x}_K^T]^T \in \mathbb{R}^{(M+L)K \times 1}$ contains the states for all time steps, and $\mathbf{Y} = [\mathbf{y}_1^T, \mathbf{y}_2^T, \dots, \mathbf{y}_K^T]^T \in \mathbb{R}^{CK \times 1}$ contains the observed measurements. The matrix \mathbf{C} is an identity matrix of size $(M+L)K \times (M+L)K$, i.e., $\mathbf{C} \equiv \mathbf{I}_{(M+L)K \times (M+L)K}$, $\mathbf{b}_* = [\mathbf{b}^T, \mathbf{0}_{(M+L)(K-1) \times 1}^T] \in \mathbb{R}^{(M+L)K \times 1}$ with $\mathbf{b} = \mathbf{x}_0$, and $\boldsymbol{\epsilon} \in \mathbb{R}^{(M+L)K \times 1}$ and $\boldsymbol{\omega} \in \mathbb{R}^{CK \times 1}$. Matrices $\mathbf{A}_* \in \mathbb{R}^{(M+L)K \times (M+L)K}$ and $\mathbf{H}_* \in \mathbb{R}^{CK \times (M+L)K}$ are block-diagonal:

$$\begin{aligned}\mathbf{A}_* &= [\mathbf{0}_{(M+L) \times (M+L)}, \text{blkdiag}(\mathbf{A}_1, \dots, \mathbf{A}_K)], \\ \mathbf{H}_* &= [\text{blkdiag}(\underbrace{\mathbf{H}, \dots, \mathbf{H}}_{K \text{ times}})],\end{aligned}$$

while $\mathbf{B}_* \in \mathbb{R}^{(M+L)K \times Q}$. To facilitate the solution of Problem (4) we define a combined vector $\mathbf{z} = [\mathbf{X}^T, \mathbf{u}^T]^T \in \mathbb{R}^{(M+L)K+Q}$ leading to:

$$\begin{aligned}\mathbf{C}_{**} \mathbf{z} + \mathbf{b}_{**} + \boldsymbol{\epsilon} &= \mathbf{0}_{(M+L)K+Q}, \\ \mathbf{Y} &= \mathbf{H}_{**} \mathbf{z} + \boldsymbol{\omega},\end{aligned}\tag{5}$$

where

$$\begin{aligned}\mathbf{C}_{**} &= [\mathbf{A}_* - \mathbf{C}, \mathbf{0}_{(M+L)K \times Q}] + [\mathbf{0}_{(M+L)K \times (M+L)K}, \tilde{\mathbf{B}}_*] \\ \mathbf{b}_{**} &= [\mathbf{b}_*^T, \mathbf{0}_{Q \times 1}^T]^T \\ \mathbf{H}_{**} &= [\mathbf{H}_*, \mathbf{0}_{C \times Q}].\end{aligned}$$

Once \mathbf{u} is obtained by solving Problem (5), the demand for each OD pair can be simply obtained by

$$\sum_{p \in \mathcal{S}_w} u_p = d_w, \quad \forall w \in \mathcal{W}.\tag{6}$$

In the next section we associate the state, observation and input vector of model (3), described in Section IV-A, with the signalised path-based CTM dynamics.

B. Problem-specific dynamics

For the definition of Model (4) under the path-based CTM we have the $(M+L)$ -state vector given by $\mathbf{x}_t = \boldsymbol{\rho}(t)$. For convenience we define $\rho_l(t) \equiv \rho_{i,p}(t)$ ⁸ such that $\boldsymbol{\rho}(t) = [\rho_1(t), \dots, \rho_l(t), \dots, \rho_M(t)]^T$ denotes the density of each candidate path $p \in \mathcal{P}_i$ in cell $i \in \mathcal{L}$ in the network at time $k \in \mathcal{T}^+$ and $M = \sum_{i \in \mathcal{L}} |\mathcal{P}_i|$. The Q average input vector \mathbf{u} , denotes the inflow of cell i at each time-step t , with $i^- \in \mathcal{E}$ and $p \in \mathcal{P}_i$.

The C -vector of observations, available from loop detectors, $\mathbf{y}_t = [\bar{\rho}_{a_1}(t), \dots, \bar{\rho}_{a_C}(t)]^T \in \mathbb{R}_+^{C \times 1}$, with $C \leq L$, $\{a_1, \dots, a_C\} \in \mathcal{C}$, are the measurements taken on a subset of (or all) cells at time $t \in \mathcal{T}^+$ and are associated with the state vector through matrix $\mathbf{H} \in \mathbb{R}^{C \times M}$. Note that \mathbf{y}_t cannot be negative and not greater than $\boldsymbol{\rho}^{max}$ hence $\mathbf{y}_t = \min\{\boldsymbol{\rho}^{max}, \max\{\mathbf{0}, \bar{\boldsymbol{\rho}}(t) + \boldsymbol{\omega}_t\}\}$.

⁸The index l maps the 2-D index $\{i, p\}$, $p \in \mathcal{P}_i$ and $i \in \mathcal{L}$, to the one-dimensional space. Assume that the upstream of cell i is characterised by a merging connection, $i^- \in \mathcal{M}$. Then the per path inflow $\varphi_i^{in}(t)$ depends on the indices $\{\tilde{j}, \tilde{p}\}$, $\tilde{p} \in \mathcal{P}_i \cap \mathcal{P}_{\tilde{j}}$, $\tilde{j} \in \mathcal{N}_i^-$ and $\{j', p\}$, $\forall j' \in \mathcal{N}_i^-$.

C. Fault model

As mentioned in Section I, sensors used to collect measurements of the density at observed links (e.g. loop detectors) are susceptible to significant disruptions due to system errors, diminishing the quality and reliability of the information they provide. The potential issues associated with traffic sensors include bias, drifting, or complete failure, all of which compromise the accuracy and dependability of the sensor measurements, yielding incorrect information. Sensor failures have to be explicitly accounted in the OD matrix estimation process to ensure efficiency and reliability.

We consider two types of potential sensor faults: (i) *additive* fault and (ii) *multiplicative* fault. For the additive fault, we have that the measurement model in Equations 3 will be given by $\mathbf{y}_t = \mathbf{H}\mathbf{x}_t + \mathbf{f}_t + \boldsymbol{\omega}_t$, where \mathbf{f}_t is the potential additive fault. For the multiplicative fault we have that $\mathbf{y}_t = (\mathbf{H} + \mathbf{F}_t)\mathbf{x}_t + \boldsymbol{\omega}_t$, where \mathbf{F}_t is the potential multiplicative fault.

V. SOLUTION APPROACH

In this section we construct mathematical formulations of the OD matrix estimation problem using the path-based CTM, with no explicit formulation of potential faulty sensors (see Section V-A) and explicit modelling of potential faulty sensors (see Section V-B).

A. Path-based CTM time-independent OD matrix estimation

As outlined in Section III-A, we use model (5) to characterize the changes in traffic density according to the path-based CTM, without consideration of faulty measurements in the problem formulation:

$$\begin{aligned} \mathbf{C}_{**}\mathbf{z} + \mathbf{b}_{**} + \boldsymbol{\epsilon} &= \mathbf{0}_{(M+L)K+Q}, \\ \mathbf{Y} &= \mathbf{H}_{**}\mathbf{z} + \boldsymbol{\omega}, \end{aligned}$$

We formulate the path-based CTM time-independent OD matrix estimation in an optimisation context as

$$\begin{aligned} \min_{\mathbf{z}} \quad & \Psi(\mathbf{z}) \\ \text{s.t.} \quad & \mathbf{z} \geq \mathbf{0}, \end{aligned} \quad (7)$$

where the objective function to be minimised is:

$$\Psi(\mathbf{z}) = \frac{1}{2} \left[\|\mathbf{Y} - \mathbf{H}_{**}\mathbf{z}\|_{[\mathbf{Z}_{\omega}]}^2 + \|\mathbf{C}_{**}\mathbf{z} + \mathbf{b}_{**}\|_{[\boldsymbol{\Sigma}_{\epsilon}]}^2 \right],$$

where $\mathbf{Z}_{\omega} = \text{blkdiag}(\mathbf{Z}_1^{\omega}, \dots, \mathbf{Z}_K^{\omega})$ and $\boldsymbol{\Sigma}_{\epsilon} = \text{blkdiag}(\boldsymbol{\Sigma}_1^{\epsilon}, \dots, \boldsymbol{\Sigma}_K^{\epsilon})$. Through formulation (7), our goal is to estimate vector \mathbf{z} by minimising the error in the objective function. However, in the case that a fault occurs on a specific sensor, we cannot identify the occurred faults, yielding lower quality OD demand estimates. We will refer to this approach as OD matrix estimation - no fault consideration, *OD-NFC*.

B. Fault-Tolerant Path-based CTM OD matrix estimation

In the presence of faulty sensors in the network, a more accurate model for describing the traffic density evolution in the path-based CTM is given by:

$$\begin{aligned} \mathbf{x}_{t+1} &= \mathbf{A}_t\mathbf{x}_t + \mathbf{B}\mathbf{u} + \boldsymbol{\epsilon}_t, \\ \mathbf{y}_t &= \mathbf{H}\mathbf{x}_t + \boldsymbol{\omega}_t + \mathbf{o}_t, \end{aligned} \quad (8)$$

where $\mathbf{o}_t = [o_{1,t}, \dots, o_{C,t}]^T$ represents the *sensor fault residuals*. Each component $o_{i,t}$ is zero if sensor $i \in \mathcal{C}$ is functioning correctly, and non-zero if sensor $i \in \mathcal{C}$ is faulty at time t [45]. The observed traffic vector \mathbf{y}_t must remain within zero and $\boldsymbol{\rho}^{\max}$, so it is adjusted to $\mathbf{y}_t = \min\{\boldsymbol{\rho}^{\max}, \max\{\mathbf{0}, \bar{\boldsymbol{\rho}}(t) + \boldsymbol{\omega}_t + \mathbf{o}_t\}\}$. Accurate recovery of the states $\bar{\boldsymbol{\rho}}(t)$ and $\boldsymbol{\rho}(t)$, as well as the fault residuals \mathbf{o}_t , is crucial for effectively estimating path demand and identifying faulty measurements. It has been demonstrated that $o_{i,t}$ is expected to have only a few non-zero entries, which leads to accurate estimation results [60].

We define a new objective function, $\Psi(\mathbf{z}, \mathbf{O})$, with respect to the new variable \mathbf{z} defined in Section V and the sensor fault residuals vector $\mathbf{O} = [\mathbf{o}_1, \dots, \mathbf{o}_K]^T$ as

$$\begin{aligned} \Psi(\mathbf{z}, \mathbf{O}) &= \frac{1}{2} \left[\|\mathbf{Y} - \mathbf{H}_{**}\mathbf{z} - \mathbf{O}\|_{[\mathbf{Z}_{\omega}]}^2 \right. \\ &\quad \left. + \|\mathbf{C}_{**}\mathbf{z} + \mathbf{b}_{**}\|_{[\boldsymbol{\Sigma}_{\epsilon}]}^2 \right], \end{aligned} \quad (9)$$

where \mathbf{Z}_{ω} and $\boldsymbol{\Sigma}_{\epsilon}$ are as defined in the previous section.

In addition, we define the *maximum sensor fault-residuals* over time, r_j , $j = 1, \dots, C$, $\forall t \in \mathcal{T}$ given by

$$r_j = \max_{t \in \mathcal{T}^+} \{|o_{j,t}|\}, \quad (10)$$

which relates a value of sensor j equal to the maximum residual $o_{j,t}$.

Using definition (10) the below convex formulation is obtained:

$$\min_{\mathbf{z}, \mathbf{O}, \mathbf{r}} \Psi(\mathbf{z}, \mathbf{O}) + \mu \sum_{j \in \mathcal{C}} r_j \quad (11a)$$

$$\text{s.t. } o_{j,t} \leq r_j, t = 1, \dots, K, j \in \mathcal{C} \quad (11b)$$

$$-o_{j,t} \leq r_j, t = 1, \dots, K, j \in \mathcal{C}, \quad (11c)$$

where $\mathbf{O} = [\mathbf{o}_1, \dots, \mathbf{o}_K]^T$, is referred to as Fault-aware OD matrix estimation, *FOD*, in the remainder of this paper. The positive regularization parameter μ in formulation (11) manages the balance between detecting faults and minimizing the optimization cost. This formulation ensures that Equations (10) are satisfied because constraints (11b)-(11c) are effectively equivalent to $\max_{t \in \mathcal{T}^+} \{|o_{j,t}|\} \leq r_j$. Meanwhile, the term $\mu \sum_{j \in \mathcal{C}} r_j$ ensures that r_j , for each $j \in \mathcal{C}$, is minimized within the feasible range, yielding (10).

C. Fault-Adaptive Path-based CTM OD matrix estimation

Although formulation (11) achieves accurate OD matrix estimation in the presence of faulty sensors, it may reduce the quality of the OD matrix under healthy operating conditions. For this reason we develop a fault-adaptive methodology, aiming to offer the best of two worlds.

Algorithm 1: Fault-adaptive OD matrix estimation

Input: \mathbf{Y} , \mathbf{C}_{**} , \mathbf{H}_{**} , \mathbf{b}_{**} , \mathbf{Z}_ω , Σ_ϵ

Solve Problem (11)

Feed $o_{j,t}$ and r_j in BEAST algorithm [52] to get change points $\tau_{j,c}$ and magnitude, m_{j,τ_c} **if** $|m_{j,\tau_c} - m_{j,\tau_{c'}}| < \delta$ **then** Correct r_j using $\frac{m_{j,\tau_c} + m_{j,\tau_{c'}}}{2}$ to get new measurement vector \mathbf{Y}_* **else** Correct r_j using $\frac{m_{j,\tau_c} - m_{j,\tau_{c'}}}{\tau_{j,c} - \tau_{j,c'}}$ to get new measurement vector \mathbf{Y}_* Solve Problem (7) using \mathbf{Y}_* Output: \mathbf{u}

The fault-adaptive algorithm developed, identifies faults and corrects the corresponding fault residuals. The procedure is given as follows. Once we have collected the measurements within the pre-specified time window under study, we solve (11) to obtain $o_{j,t}$ and r_j , $\forall t \in \mathcal{T}^+$ and $j \in \mathcal{C}$. Then, the fault residuals, $o_{j,t}$, are fed in the BEAST algorithm [52] to obtain the change points, $\tau_{j,c}$ with $c = 1, \dots, D$ and D the total number of identified change points, if they exist along with their corresponding magnitude, m_{j,τ_c} , $\tau_c \in \mathcal{F}_j$, where \mathcal{F}_j indicates the faulty time window of sensor $j \in \mathcal{C}$. For each pair of change points we calculate their difference. If this difference is below a pre-specified threshold δ , we assume an additive fault has occurred and the faulty sensor measurements are compensated according to the two fault magnitudes' average value. If the difference is above the pre-specified threshold δ , we assume we assume a multiplicative fault has occurred which we compensate using the slope between the two change-points. In both cases, the faulty sensor measurements are compensated in \mathcal{F}_j and the OD matrix estimation problem is solved with no consideration of faulty sensors, i.e. solve Problem (7). This procedure is outlined in Algorithm 1 and is referred to as FOD_{corr} . An alternative strategy for robust OD matrix estimation involves disregarding the measurements from the faulty sensor within the faulty time window \mathcal{F}_j , rather than attempting to correct them, referred to as FOD_{ign} . These two variants are thoroughly investigated in Section VI.

VI. PERFORMANCE EVALUATION

To evaluate the performance of the proposed OD matrix estimation methodology under faulty measurements we examine two real life networks: (i) an abstraction of Leicesters' traffic network [5], consisting of 9 OD pairs and each OD pair has 2-4 paths over which the OD flows are distributed, and (ii) the Nguyen-Dupuis network [61] that was extensively used as a case study in many works (see for example [59], [62]), consisting of 20 OD pairs and 70 total paths.

Two types of loop detector layouts are considered:

- *Full coverage:* All cells within the network are equipped with loop detectors, hence $C = L$, representing full (100%) coverage of the network's cells.

- *Random partial coverage:* Loop detectors are distributed unevenly across the network, where $C < L$. In this case, detectors are randomly removed from certain cells, resulting in three distinct coverage scenarios: 80%, 60%, and 40% of the total cells.

We built a simulator of the proposed path-based CTM (Section III-A), that takes as inputs the boundary conditions of each cell. The output of the simulator is the measured density for each cell used as the state space model measurements. We employ the framework for OD estimation under faulty measurements (Section V-B), FOD, and compare estimation results using the formulation that does explicitly considers faulty sensors in the formulation, OD-NFC (Section V-A). In addition, we employ the fault-adaptive algorithm described in Section V-C and examine the OD matrix estimation performance when correcting or ignoring faulty measurements. To obtain the estimation results we vary the number of faulty sensors in the network as well as their fault magnitude. To evaluate the performance of each OD estimation algorithm, we use two key metrics: the root mean squared error (RMSE) and the mean absolute percentage error (MAPE), defined as follows:

$$\text{OD}_{\text{RMSE}} = \sqrt{\frac{1}{W} \sum_{w=1}^W (d_w^{\text{true}} - d_w)^2}, \quad (12a)$$

$$\text{OD}_{\text{MAPE}} = \frac{1}{W} \sum_{w=1}^W \frac{|d_w^{\text{true}} - d_w|}{d_w^{\text{true}}} 100\%, \quad (12b)$$

where W is the total number of OD pairs, d_w^{true} is the true OD demand considered during the simulation and d_w is the estimated OD demand. Further, we investigate the effect of the positive regularisation parameter μ (see Problem (11)) with respect to estimating both the OD matrix of interest as well as the maximum fault residual errors. We present results for different values of μ assuming a fixed faulty scenario and calculate the average RMSE of the OD demand, OD_{RMSE} , given in (12a), and the RMSE of the maximum of the fault residuals error, RES_{RMSE} , given by

$$\text{RES}_{\text{RMSE}} = \sqrt{\frac{1}{C} \sum_{i=1}^C (r_i - \hat{r}_i)^2}, \quad (13)$$

where C is the total number of measured cells, r_i is the true maximum fault residual of sensor i considered during the simulation and \hat{r}_i is the estimated maximum fault residual of sensor i .

In both experiments, we assume that the measurements and the model are influenced by Gaussian noise, with the noise having a zero mean. The variance of the model noise and measurement noise are represented by $\sigma_\epsilon^2 \mathbf{I}$ and $\sigma_\omega^2 \mathbf{I}$, respectively. We set the model variance $\sigma_\epsilon^2 = 3$ and the measurement variance $\sigma_\omega^2 = 3$. Also, we consider that at each time step the path-based demand vector is generated from the normal distribution $\mathcal{N}(\bar{\mathbf{u}}, \Sigma)$, where $\bar{\mathbf{u}}$ is a constant unknown path-demand vector and Σ is a diagonal covariance matrix such that $\text{diag}(\Sigma)^{1/2} = 0.1\bar{\mathbf{u}}$.

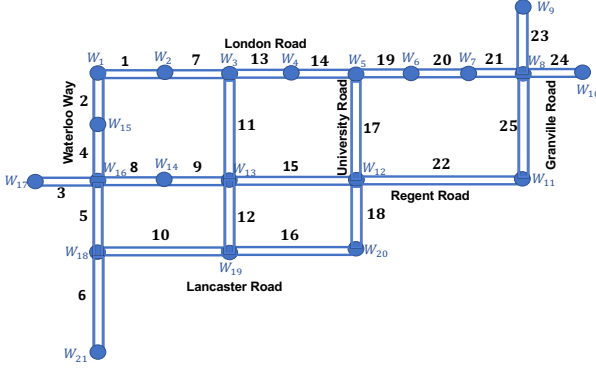


Fig. 2: Leicester network.

A. Simulation Experiment I: Leicester network

For the first simulation experiment we assume the Leicester network given in Figure 2, which consists of 25 cells, 25 pre-specified paths and 9 OD pairs. Traffic enters the network from the upstream boundary of cells 1, 2, 3 and 23 and exits from the downstream boundary of cells 6, 16, 18, 24 and 25. In addition, we consider the following CTM parameter values (we assume that all cells have equal conditions): $v_i^f = 60$ km/h, $v_i^b = 20$ km/h, $\varphi_i^{max} = 1500$ veh/h, $\rho_i^{max} = 100$ veh/km, $\rho_i^c = 25$ veh/km and $l_i \in [0.15, 0.40]$ km. The predefined time period of study is $T = 2$ hours and we assume that $T_s = 10$ seconds and hence we observe measurements for $K = 720$ intervals.

Initially, we investigate the effect of the positive regularisation parameter μ (see Problem (11)) with respect to estimating both the OD matrix of interest as well as the maximum fault residual errors. We assume that we have measurements on all cells of the network i.e. all cells are equipped with loop detectors that provide measurements of the link density. We run the simulator and collect density measurements when there is one faulty sensor in the network, $n_f = 1$. We assume an additive error on sensor 6 and fault magnitude 14 veh/km for period $t \in [600, 700]$. Results for Problem (11), shown in Figure 3 suggest that there is a trade off between detecting faults and optimising cost. We aim to minimise both OD_{RMSE} and $RMSE_{res}$ and Figure 3 suggests that there is a sweet spot of values for μ , $\mu \in [10^{0.5}, 10^{-1.5}]$, where we can achieve this.

Next, we investigate the performance of the proposed methodology with respect to the accuracy of estimating the OD demand, as well as the faulty sensors and their fault magnitude simultaneously, assuming full or random partial coverage of the network. In addition, we investigate the efficiency of the approach with respect to different fault magnitudes and number of faults. Note that in the reminder of this paper we set the tuning parameter to $\mu = 10^{0.5}$. In the subsequent experiments, each optimization procedure is executed 50 times. During each execution, a different subset of cells is chosen to either produce faulty measurements, or to exclude their measurements, particularly in the case of random partial coverage, and varying fault magnitudes in the range $[0.5, 10]$ veh/km, to mitigate potential biases

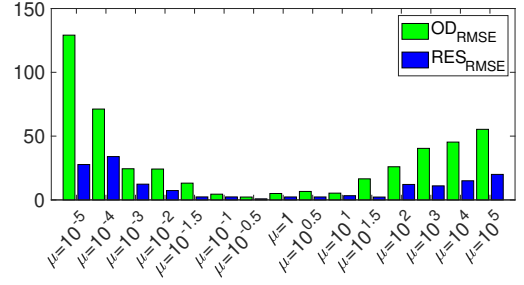


Fig. 3: Root Mean Squared error for different values of the μ (see Problem (11)) of parameter estimation (green) and squared error of fault residual parameter values (blue) for $n_f = 1$ for the time window $T = 2$ hours.

Cov.	n_f	OD-NFC		FOD	
		OD_{RMSE} [veh/h]	OD_{MAPE} [%]	OD_{RMSE} [veh/h]	OD_{MAPE} [%]
100%	0	5.54±0.62	3.1±0.1	3.93±0.20	3.6±0.2
	2	21.08±3.05	15.8±2.1	5.62±0.59	4.1±0.2
	4	33.48±5.95	19.3±3.0	6.94±0.75	10.4±1.3
	6	99.77±9.87	37.2±6.4	13.07±2.41	15.9±2.9
	8	123.12±10.17	45.2±6.8	25.54±4.98	33.9±5.4
80%	0	9.28±2.67	7.5±1.7	6.87±0.96	4.3±0.8
	2	57.52±7.12	15.5±2.9	20.24±3.56	14.2±1.9
	4	86.74±8.86	22.3±3.9	28.15±4.03	14.8±2.2
	6	147.86±12.03	46.2±6.2	33.36±5.97	21.8±3.7
60%	0	15.21±2.21	10.1±2.06	16.12±2.81	12.4±1.9
	2	182.15±15.77	31.83±5.3	34.91±5.62	15.2±2.5
	4	263.69±17.61	67.03±7.2	83.38±8.18	37.9±5.9
	6	301.69±20.31	71.25±8.0	99.97±8.54	41.2±6.1
40%	0	38.91±5.87	9.5±1.5	38.21±6.23	10.9±1.4
	2	296.34±18.67	61.1±7.12	89.92±8.99	36.0±6.0
	4	378.99±23.42	80.7±9.2	103.67±9.68	40.5±6.9

TABLE I: Average OD_{RMSE} and average OD_{MAPE} for different network coverage (Cov.) and different number of faulty measurements using the OD-NFC and FOD solution approaches.

in the results, ensuring a robust evaluation of the proposed methodology.

In Table I, we present the average values for OD_{RMSE} and OD_{MAPE} , and the standard deviation of the different runs of the optimisation procedure, obtained through the application of OD-NFC and FOD approaches under different network coverage scenarios (full and random partial loop detector layouts). Both metrics are calculated for varying numbers of faulty sensors in each network coverage case, highlighting the efficacy of our proposed solution approach in OD matrix estimation when faulty sensors are present in the network. Both formulations should be equivalent when there are no faulty sensors in the network, as evident from the results, where for $n_f = 0$ the OD_{RMSE} and OD_{MAPE} are very similar for the two formulations. As expected, increasing the number of faulty sensors yields higher values for both metrics, however, across all cases, the FOD solution approach consistently outperforms the OD-NFC approach, demonstrating its superiority in producing more accurate results. Specifically, the FOD approach exhibits results that are up to 5 times better than those obtained with the OD-NFC approach in terms of OD_{RMSE} . Nevertheless, the FOD solution approach consistently delivers more accurate

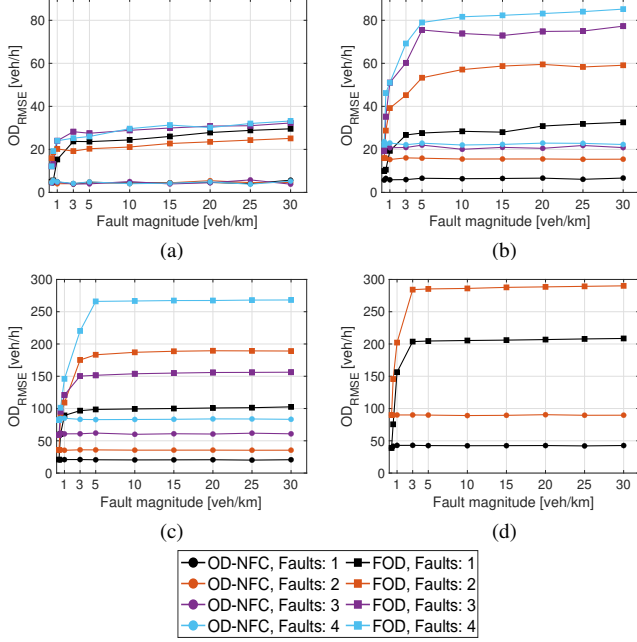


Fig. 4: Average OD_{RMSE} for different fault magnitudes for the OD-NFC and FOD approaches, and (a) 100%, (b) 80%, (c) 60% and (d) 40% network coverage.

results even under such challenging conditions. Further, the standard deviation values show that the variability of the optimisation results becomes larger as we decrease the percentage of network coverage suggesting that different subsets of measured road segments may be subject to larger estimation error. However, for both networks the standard deviation is less than 10% of the average value, indicating robust results under different settings of the experiment.

Next we thoroughly assess the performance of the proposed approach and provide insights of its effectiveness across diverse network coverage scenarios and under different faulty conditions. Towards this, we consider varying faulty magnitudes for each network coverage scenario and investigate the robustness of the proposed approach. Figure 4 illustrates the average OD_{RMSE} for both the OD-NFC and FOD methods at different percentages of network coverage. Specifically, Figure 4 (a) corresponds to 100% network coverage, Figure 4 (b) to 80%, Figure 4 (c) to 60%, and Figure 4 (d) to 40% network coverage. Notably, when the fault magnitude is small (e.g., 0.3), both methods yield similar results. This may be attributed to the fact that both approaches may treat such small magnitudes as measurement or model errors rather than significant disturbances. However, these minor errors have a negligible impact on the estimation performance, as evident from Figure 4 and Table I. Overall, the FOD approach demonstrates lower variation in the results as the fault magnitude increases, while the OD-NFC approach exhibits an increasing trend under similar conditions. This observation suggests that the FOD approach maintains a more consistent performance across varying fault magnitudes.

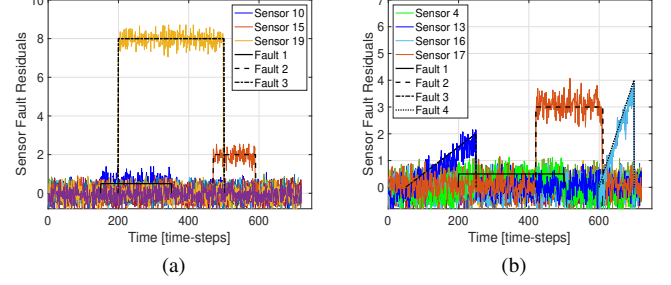


Fig. 5: Fault residual parameter values with (a) $n_f = 3$ and (b) $n_f = 4$.

To demonstrate the effectiveness of the FOD approach in varying fault scenarios, we collected measurements with full network coverage under two different conditions as follows. (i) Three faulty sensors, $n_f = 3$: We introduced faults in sensors 10, 15, and 19, with magnitudes of 0.5 veh/km, 2 veh/km, and 8 veh/km, respectively. The faults occurred during the following time periods: $t \in [150, 350]$, $t \in [470, 590]$, and $t \in [200, 500]$, respectively. (ii) Four faulty sensors, $n_f = 4$: Faults were applied to sensors 4 and 17 with magnitudes 0.5 veh/km and 3 veh/km for periods $t \in [200, 500]$ and $t \in [420, 610]$, respectively. Additionally, sensors 13 and 16 experienced multiplicative errors, with factors $t/60$ and $t/20$, respectively, during periods $t \in [50, 250]$ and $t \in [600, 700]$.

Figure 5 illustrates the results, where the x -axis represents time (with $K = 720$ time steps corresponding to $T = 2$ hours) and the y -axis shows the sensor fault residuals ($o_{i,t}; i \in C$). The figure indicates that most fault residuals are close to zero, suggesting effective fault detection. The non-zero residuals are attributable to model and measurement noise. For the faulty sensors, the proposed method successfully identifies faults, as evidenced by the significant increase in fault residuals for sensors 10, 15, and 19 during their fault periods, accurately tracking the magnitude of these faults (Figure 5 (a)). Similarly, Figure 5 (b) demonstrates that the approach accurately detects both additive and multiplicative faults, with noticeable increases in fault residuals for sensors 4, 13, 16, and 17 during their fault periods. For both cases the OD_{RMSE} remains low as indicated in Table I.

Finally, we focus on evaluating the fault-adaptive OD matrix estimation algorithm (Algorithm 1). Specifically, we aim to explore the impact of correcting or ignoring faulty measurements, assuming either full or random partial coverage of the network. In Table II we present average values for both OD_{RMSE} and OD_{MAPE} for the two variants of the fault-adaptive approach, namely FOD_{ign} and FOD_{corr} (see Section V-C), across various network coverage configurations, including full and random partial loop detector layouts, along with the standard deviation of the different runs of the procedure. We vary the number of faulty sensors in each network coverage scenario to provide a more in-depth understanding of the algorithm. Notably, when dealing with

Cov.	n_f	FOD_{ign}		FOD_{corr}	
		OD _{RMSE} [veh/h]	OD _{MAPE} [%]	OD _{RMSE} [veh/h]	OD _{MAPE} [%]
100%	1	5.69±0.57	9.1±1.1	5.92±0.59	4.4±0.4
	2	9.73±1.36	12.8±1.7	6.74±0.81	5.3±0.6
	4	11.58±1.47	13.4±2.0	7.02±1.93	7.3±0.9
	6	16.48±2.06	15.2±2.1	9.25±1.47	7.9±0.9
	8	37.99±6.93	20.5±3.1	10.19±1.82	9.0±1.4
80%	1	19.93±2.91	15.5±2.0	12.71±1.69	6.2±0.7
	2	20.61±2.82	16.4±2.2	10.49±1.92	7.9±1.0
	4	22.82±2.99	20.0±3.2	13.22±1.19	8.2±1.3
	6	26.79±3.45	23.4±4.1	14.99±1.33	13.8±1.2
	8	26.79±3.45	23.4±4.1	14.99±1.33	13.8±1.2
60%	1	12.87±3.11	9.3±1.2	6.07±0.73	4.2±0.3
	2	18.42±2.81	16.3±2.8	11.64±1.54	8.6±1.7
	4	22.45±3.23	20.0±3.3	15.14±2.97	10.7±2.2
	6	26.44±3.75	24.2±3.9	17.34±3.12	15.2±1.4
	8	26.44±3.75	24.2±3.9	17.34±3.12	15.2±1.4
40%	1	18.82±2.92	14.8±2.8	7.76±1.94	6.3±0.8
	2	27.57±3.94	18.7±3.0	12.92±1.67	7.7±1.6
	4	27.57±3.94	18.7±3.0	12.92±1.67	7.7±1.6
	6	47.13±6.06	41.2±7.1	14.04±1.89	9.3±1.8
	8	47.13±6.06	41.2±7.1	14.04±1.89	9.3±1.8

TABLE II: Average OD_{RMSE} and average OD_{MAPE} for different network coverage and different number of faulty measurements using the OD-NFC and FOD solution approaches.

a limited number of faults and complete network coverage, both approaches yield very similar results. However, as the number of faults increases under conditions of random partial network coverage, results indicate that correcting faulty measurements yields results that are up to three times more accurate. This supports the effectiveness of the fault adaptive OD estimation approach, particularly in scenarios with random partial coverage and high number of faults, demonstrating its capability to enhance estimation accuracy through targeted correction mechanisms. As before, the standard deviation values are about 10% of the average value, indicating robust results under the two variants of the fault adaptive OD matrix estimation algorithm.

Table III is the confusion matrix indicating the number of true positives, false negatives, false positives, and true negatives in terms of fault identification of the proposed fault-adaptive algorithm. To obtain these results we assume various network coverage configurations, including full and random partial loop detector layouts and vary the number of faulty sensors and fault magnitudes in each network coverage scenario. Under these conditions we run 50 different simulations across all different scenarios. As shown in Table III, the proposed approach is able to correctly identify faults. Notably, even for a small percentage of network coverage and a large number of faults, the proposed fault adaptive methodology significantly improves the OD estimation accuracy as shown in Tables I-II.

B. Simulation Experiment II: Nguyen-Dupuis network

The entire framework is also applied to a larger network, the Nguyen-Dupuis network [61] that was extensively used as a case study in many works (see for example [59], [62]), shown in Figure 6. This network consists of 65 cells, 20 OD pairs and 70 pre-specified paths. The following CTM parameters are considered: $v_i^f = 60$ km/h, $v_i^b = 20$ km/h, $\varphi_i^{max} = 1500$ veh/h, $\rho_i^{max} = 100$ veh/km, $\rho_i^c = 25$ veh/km, $l_i \in [0.3, 0.8]$ km. The predefined time period of study is $T = 2$ hours and the time step is $T_s = 10$ seconds and hence we observe measurements for $K = 720$ intervals.

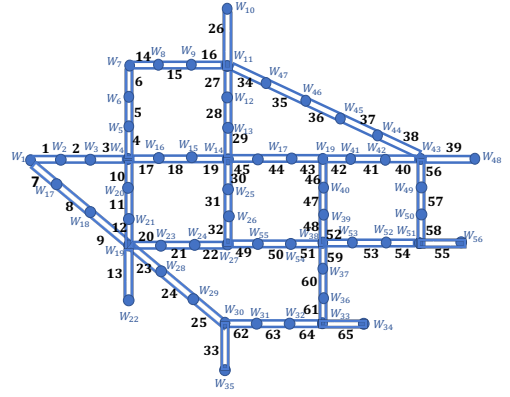


Fig. 6: Nguyen-Dupuis network.

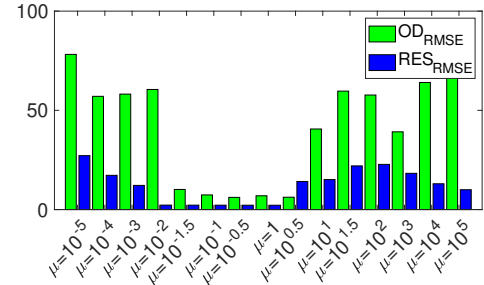


Fig. 7: Root Mean Squared error for different values of the μ (see Problem (11)) of parameter estimation (green) and squared error of fault residual parameter values (blue) for $n_f = 4$ for the time window $T = 2$ hours.

As for the previous network, we investigate the effect of the positive regularisation parameter μ (see Problem (11)) with respect to estimating both the OD matrix of interest as well as the maximum fault residual errors. We present results for different values of μ assuming a fixed faulty scenario and calculate the average RMSE of the OD demand, OD_{RMSE}, given in (12a), and the average RMSE of the maximum of the fault residuals error, given in (13). We assume that we have measurements on all cells of the network i.e. all cells are equipped with loop detectors that provide measurements of the link density. We run the simulator and collect measurements when there are four faulty sensors in the network, $n_f = 4$. Results for Problem (11), shown in Figure 7 suggest that there is a trade off between detecting faults and optimising cost. We aim to minimise both OD_{RMSE} and RMSE_{res} and Figure 7 confirms the previous findings that there is a sweet spot of values for μ , $\mu \in [10^{0.5}, 10^{-2}]$, where we can achieve this. Hence we set $\mu = 10^{0.5}$ for the remainder of this section.

Next, we investigate the performance of the proposed methodology with respect to the accuracy of estimating the OD demand, as well as the faulty sensors and their fault magnitude simultaneously, assuming full or random partial coverage of the network. Additionally, we evaluate the fault-adaptive OD matrix estimation algorithm (Algorithm 1) to understand how correcting or ignoring faulty measurements affects the outcomes, under conditions of both full and

Actual		Predicted							
		100% network coverage		80% network coverage		60% network coverage		40% network coverage	
		Faulty	Not Faulty	Faulty	Not Faulty	Faulty	Not Faulty	Faulty	Not Faulty
	$n_f = 0$	Faulty	TP=99.2% FN=0.8%	Faulty	TP=97.8% FN=2.2%	Faulty	TP=95.4% FN=4.6%	Faulty	TP=94.3% FN=5.7%
		Not Faulty	FP=0.1% TN=99.9%	Not Faulty	FP=1.3% TN=98.7%	Not Faulty	FP=2.6% TN=97.4%	Not Faulty	FP=4.2% TN=95.8%
	$n_f = 2$	Faulty	TP=98.9% FN=1.1%	Faulty	TP=96.2% FN=3.8%	Faulty	TP=94.2% FN=5.8%	Faulty	TP=93.1% FN=6.9%
		Not Faulty	FP=1.5% TN=98.5%	Not Faulty	FP=2.9% TN=97.1%	Not Faulty	FP=3.8% TN=96.2%	Not Faulty	FP=4.9% TN=95.1%
	$n_f = 4$	Faulty	TP=97.3% FN=2.7%	Faulty	TP=95.9% FN=4.1%	Faulty	TP=93.1% FN=6.9%	Faulty	TP=91.8% FN=8.2%
		Not Faulty	FP=2.6% TN=97.4%	Not Faulty	FP=3.9% TN=96.1%	Not Faulty	FP=6.1% TN=93.9%	Not Faulty	FP=7.7% TN=92.3%
	$n_f = 6$	Faulty	TP=95.4% FN=4.6%	Faulty	TP=94.4% FN=5.6%	Faulty	TP=92.2% FN=7.8%	Faulty	TP=91.0% FN=9.0%
		Not Faulty	FP=4.0% TN=96.0%	Not Faulty	FP=4.2% TN=95.8%	Not Faulty	FP=6.3% TN=93.7%	Not Faulty	FP=7.5% TN=93.5%

TABLE III: Confusion matrix for the proposed fault-adaptive algorithm for the Leicester network.

Cov.	n_f	OD-NFC		FOD		FOD _{ign}		FOD _{corr}	
		ODRMSE [veh/h]	ODMAPE [%]	ODRMSE [veh/h]	ODMAPE [%]	ODRMSE [veh/h]	ODMAPE [%]	ODRMSE [veh/h]	ODMAPE [%]
100%	0	2.19±0.22	14.3±2.1	3.03±0.28	16.7±2.8	3.29±0.34	14.6±2.4	2.85±0.27	11.9±1.9
	2	7.82±0.91	34.3±6.5	5.52±0.68	25.3±3.5	3.94±0.35	14.2±1.7	3.46±0.34	16.1±2.7
	4	57.02±7.32	43.0±6.1	8.51±1.11	37.4±6.8	5.01±0.55	16.6±1.9	4.17±0.43	17.7±1.5
	8	68.91±5.99	46.1±4.1	13.90±1.81	37.8±6.4	5.27±0.63	17.1±1.9	4.49±0.38	18.5±1.9
	16	100.84±9.87	63.7±5.6	33.82±3.92	46.1±3.9	28.35±2.73	23.9±2.1	7.91±0.92	20.8±2.1
80%	0	4.12±0.35	21.8±2.3	8.70±1.34	27.0±2.4	4.54±0.39	20.7±2.1	4.34±0.31	17.1±1.6
	2	13.87±2.87	31.7±3.0	9.62±1.46	29.9±3.9	4.92±0.42	22.8±2.9	5.02±0.71	21.8±1.9
	4	73.69±8.92	41.1±4.2	11.41±1.62	34.0±4.2	5.19±0.59	35.3±3.8	5.79±0.57	23.1±2.8
	8	97.81±9.26	56.5±5.1	19.85±2.01	40.3±4.8	21.48±2.62	38.6±3.1	6.51±0.77	27.0±2.6
	16	124.85±11.78	69.6±7.0	25.66±2.45	45.1±4.1	91.79±8.99	42.5±4.4	9.41±2.02	25.8±2.9
60%	0	15.57±1.53	29.4±3.3	19.16±2.03	27.8±3.0	14.06±1.83	22.4±2.8	12.68±1.45	18.8±3.8
	2	26.26±2.22	36.3±2.9	19.39±2.08	30.7±3.2	21.13±2.71	23.5±2.6	13.70±1.46	21.3±2.1
	4	81.68±7.78	45.5±3.8	25.58±2.66	44.4±4.7	24.25±2.33	23.9±2.3	18.82±2.05	28.0±3.0
	8	102.59±10.42	60.5±5.9	30.14±2.98	58.5±5.5	28.47±3.02	30.8±3.2	22.57±2.08	32.1±3.3
	16	207.36±19.17	72.3±6.8	42.14±4.87	59.9±5.1	101.22±9.35	67.3±5.9	27.32±2.69	39.5±4.0
40%	0	32.51±3.09	26.0±2.2	39.11±4.03	36.3±3.4	33.16±2.98	28.4±2.7	34.25±3.67	23.9±2.2
	2	50.09±4.99	47.7±4.8	42.60±4.31	42.2±4.0	35.16±3.39	31.4±3.7	41.79±4.08	24.0±2.5
	4	101.48±9.88	60.3±5.6	54.72±6.68	45.6±4.7	65.97±7.56	49.5±5.0	43.03±4.09	28.8±3.4
	8	150.73±13.87	78.8±9.0	67.57±5.99	50.5±4.9	95.51±9.09	71.8±6.6	48.37±5.03	34.0±3.3

TABLE IV: Average ODRMSE and average ODMAPE for different network coverage and different number of faulty measurements using the OD-NFC, FOD, FOD_{ign} and FOD_{corr} approaches.

random partial network coverage. Each experiment involves running both optimization procedures 50 times, with a different subset of cells selected for faulty measurements or ignored measurements (in the case of random partial coverage) in each run, to reduce potential biases and ensure a comprehensive assessment of the proposed methodology. Table IV summarizes the average ODRMSE and ODMAPE values for the OD-NFC and FOD methods across different network coverage scenarios (full and random partial loop detector layouts). It also includes results for the two variants of the fault-adaptive approach, FOD_{ign} and FOD_{corr}, across various network coverage configurations, along with the standard deviation of the 50 runs of the optimisation procedure.

As shown in Table IV all formulations should be equivalent when there are no faulty sensors in the network, with the FOD approach yielding slightly lower ODRMSE and ODMAPE than the other three formulations. As expected, increasing the number of faulty sensors all approaches exhibit larger estimation error, however, across all cases, the FOD_{corr} solution approach consistently outperforms both the OD-NFC and the FOD_{ign} approach. Specifically, the FOD approach exhibits results that are up to 5 times better than those obtained with the OD-NFC approach in terms of ODRMSE, while the FOD_{ign} approach improves the estimation accuracy up to up to 75% and the FOD_{corr} approach up to 87%. Note that the two variants of the fault-

adaptive algorithm yield similar results for high percentages of network coverage, however for low percentage of network coverage or a high number of faults we can conclude that the most robust results are obtained by utilising the FOD_{corr} approach. Similar to the previous experiment, the standard deviation values are about 10% of the average value, indicating robust results under all formulations.

We compare the estimation performance of the OD-NFC, FOD, FOD_{ign} and FOD_{corr} approaches for different percentages of network coverage and varying number of faulty sensors. In Figure 8 we present the estimated OD demands against the true OD demands and calculate the R^2 given by

$$R^2 = 1 - \frac{d_w^{\text{true}} - d_w}{d_w^{\text{true}} - \bar{d}}.$$

The simulations assume an 80% random partial coverage, and the optimization procedure is repeated 50 times, each time considering a different number of faults. The presented results highlight significant differences in the estimation accuracy among the approaches. Notably, the OD-NFC approach demonstrates lower R^2 values compared to the other methods, indicating a higher discrepancy between estimated and true OD demands. The consideration of faulty measurements in the formulation, as in the FOD approach, leads to improved estimation results. Moreover, by employing the fault-adaptive algorithm, the FOD_{corr} approach outperforms the other methods, achieving the highest accuracy in esti-

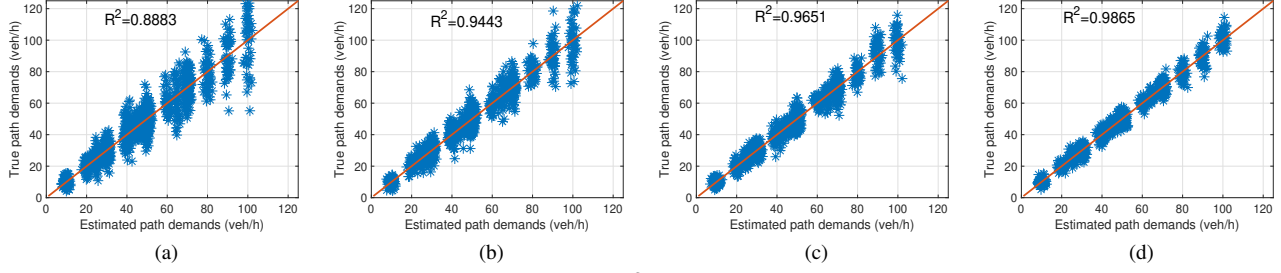


Fig. 8: Estimated, \mathbf{d} , against true, \mathbf{d}^{true} , OD demands and R^2 of the OD demands for 80% random partial network coverage for: (a) OD-NFC, (b) FOD, (c) FOD_{ign} (d) FOD_{corr}.

imating OD demands. These findings are consistent with the results presented in Table IV, reinforcing the effectiveness of the FOD_{corr} approach in enhancing estimation accuracy, especially in scenarios involving partial network coverage and varying number of sensor faults.

Finally, we assess the estimation accuracy of the proposed fault-adaptive algorithm. Table V is the confusion matrix indicating the number of true positives, false negatives, false positives, and true negatives for the Nguyen-Dupuis network, obtained following the same procedure as for the Leicester network. As shown in Table V, the proposed approach yields results with high accuracy in fault identification, while most importantly, the proposed fault adaptive methodology significantly improves the OD estimation accuracy as shown in Table IV.

VII. DISCUSSION

This work presents a novel model-based methodology for estimating OD matrices using fine-grained traffic counts collected from stationary sensors distributed across the network, even when these sensors may experience faults. A key innovation of our approach lies in its explicit handling of faulty sensor data, including the detection, isolation, and correction of these faults - an aspect that has not been explored in the context of OD matrix estimation. In this context, two additional contributions emerge: (i) the extension of our previously introduced path-based OD matrix estimation framework from [22] to account for both measurement and model noise, and (ii) the identification of sensor faults, along with the correction of faulty measurements. Moreover, the problem formulation, which utilizes fine-grained measurements, introduces several important advantages: (i) it requires no prior or target OD matrices, avoiding the biases and dependencies associated with them, (ii) it eliminates the need for route choice models or split ratios, (iii) it does not rely on user equilibrium assumptions for accurate estimation, (iv) it does not require historical data, and (v) it delivers high-quality OD matrix estimates even with partial network coverage.

A current limitation of this work is that the proposed methodology only addresses networks operating under free-flow conditions. As part of future research, we aim to extend the approach to incorporate networks operating under con-

gested conditions. This extension will involve a generalized nonlinear state-space model described by:

$$\begin{aligned} \mathbf{x}_{t+1} &= \mathbf{f}(\mathbf{x}_t, \mathbf{u}) + \boldsymbol{\epsilon}_t \\ \mathbf{y}_t &= \mathbf{H}\mathbf{x}_t + \boldsymbol{\omega}_t + \mathbf{o}_t, \end{aligned} \quad (14)$$

where $\mathbf{f}(\cdot, \cdot)$ represents the nonlinear traffic dynamics, such as those found in macroscopic models. The challenge of solving this problem arises from the high dimensionality of the state vector \mathbf{x}_t that must be estimated at each time step, along with the nonlinearity of the dynamics, which result in a challenging non-convex optimisation formulation. To address this, we plan to explore two custom optimization approaches: (i) a successive convexification technique that iteratively constructs tighter convex bounding sets for all nonlinear terms, and (ii) a successive linearization approach that approximates nonlinear terms with linear counterparts around the current solution.

VIII. CONCLUSIONS AND FUTURE WORK

This paper explores the estimation of OD matrices in the presence faulty measurements, an area that has not been addressed in existing literature. The path-based CTM OD matrix estimation method, which incorporates fault considerations into OD matrix estimation, shows significant improvements compared to approaches that do not explicitly account for faults. The model-based technique used for OD matrix estimation proves to be effective, delivering precise OD matrix estimates and demonstrating strong capabilities in detecting and identifying faulty sensors. The fault-adaptive algorithm considered was showcased to further improve the accuracy of the OD matrix estimation, especially when faulty measurements are corrected within their faulty window, to conclude that an efficient approach that identifies, isolates and compensates faulty measurements can improve the estimation performance up to 80%. A systematic investigation allowed us to thoroughly assess the performance and applicability of the proposed approach, providing insights into its effectiveness across diverse network coverage scenarios and under different fault conditions. The consideration of varying fault magnitudes and numbers of faults enhances the applicability of this methodology in real-world scenarios, making it a robust and adaptive solution for accurate OD demand estimation and fault detection

		Predicted							
		100% network coverage		80% network coverage		60% network coverage		40% network coverage	
Actual	Faulty	Faulty	Not Faulty	Faulty	Not Faulty	Faulty	Not Faulty	Faulty	Not Faulty
	Not Faulty	TP=98.2%	FN=1.8%	TP=96.8%	FN=3.2%	TP=94.3%	FN=5.7%	TP=93.1%	FN=6.9%
		FP=1.1%	TN=98.9%	FP=3.3%	TN=96.7%	FP=4.5%	TN=95.5%	FP=5.7%	TN=94.3%
	Faulty	TP=96.9%	FN=3.1%	TP=94.2%	FN=5.8%	TP=92.8%	FN=7.2%	TP=91.6%	FN=8.4%
	Not Faulty	FP=4.5%	TN=95.5%	FP=4.9%	TN=95.1%	FP=4.9%	TN=95.1%	FP=6.5%	TN=93.5%
	Faulty	TP=95.3%	FN=4.7%	TP=93.9%	FN=6.1%	TP=91.9%	FN=8.1%	TP=90.9%	FN=9.1%
	Not Faulty	FP=5.6%	TN=94.4%	FP=5.9%	TN=94.1%	FP=6.1%	TN=93.9%	FP=7.7%	TN=92.3%
	Faulty	TP=93.4%	FN=6.6%	TP=91.4%	FN=8.6%	TP=91.0%	FN=9.0%	TP=90.1%	FN=9.9%
	Not Faulty	FP=6.3%	TN=93.7%	FP=7.2%	TN=92.8%	FP=7.6%	TN=92.4%	FP=8.8%	TN=91.2%

TABLE V: Confusion Matrix for fault identification of the fault-adaptive algorithm for the Nguyen-Dupuis network.

in transportation systems. In summary, the proposed FOD solution approach appears as a robust and superior method for OD estimation in the presence of faulty measurements.

Future research will focus on adapting the proposed methodology to handle networks experiencing congestion, as described in Section VII. Additionally, there is potential to refine this approach for dynamic OD matrix estimation.

REFERENCES

- [1] S. Bera and K. V. K. Rao, "Estimation of origin-destination matrix from traffic counts: the state of the art," *European Transport*, vol. 49, pp. 3–23, 2011.
- [2] T. Toledo, T. Kolehkhina, P. Wagner, B. Ciuffo, C. Azevedo, V. Marzano, and G. Flötteröd, *Traffic Simulation and Data: Validation methods and applications*. London: CRC Press, Taylor and Francis, 2015, ch. Network model calibration studies, pp. 141–162.
- [3] C. Tebaldi and M. West, "Bayesian inference on network traffic using link count data (with discussion)," *Journal of American Statistical Association*, vol. 93, pp. 557–576, 1998.
- [4] B. Li, "Bayesian inference for origin-destination matrices of transport networks using the EM algorithm," *Technometrics*, vol. 47, pp. 399–408, 2005.
- [5] M. L. Hazelton, "Bayesian inference for network-based models with a linear inverse structure," *Transportation Research Part B*, vol. 44, pp. 674–685, 2010.
- [6] L. De Grange, F. Gonzalez, and S. Bekhor, "Path flow and trip matrix estimation using link flow density," *Networks and Spatial Economics*, vol. 17, pp. 173–195, 2017.
- [7] Y. Englezou, S. Timotheou, and C. G. Panayiotou, "Bayesian estimation of the origin-destination matrix using traffic flow dynamics," in *IEEE Intelligent Transportation Systems Conference (ITSC)*, Auckland, New Zealand, 2019, pp. 2545–2550.
- [8] M. J. Maher, "Inferences on trip matrices from observations on link volumes: A Bayesian statistical approach," *Transportation Research Part B*, vol. 17, pp. 435–447, 1983.
- [9] X. Zhou and H. S. Mahmassani, "A structural state space model for realtime traffic origin-destination demand estimation and prediction in a day-to-day learning framework," *Transportation Research Part B*, vol. 41, pp. 823–840, 2007.
- [10] E. M. Airolidi and A. W. Blocker, "Estimating latent processes on a network from indirect measurements," *Journal of American Statistical Association*, vol. 108, pp. 149–164, 2013.
- [11] L. Ying, J. Zhu, W. Huiyan, and L. Zhenyu, "A novel method for estimation of dynamic OD flow," *Procedia Engineering*, no. 137, pp. 94–102, 2016.
- [12] W. Ma and Z. Qian, "Estimating multi-year 24/7 origin-destination demand using high-granular multi-source traffic data," *Transportation Research Part C: Emerging Technologies*, vol. 96, pp. 96–121, 2018.
- [13] M. Bell, "The estimation of origin-destination matrices by constrained generalized least squares," *Transportation Research B*, vol. 25, pp. 13–22, 1991.
- [14] E. Cascetta, A. Papola, V. Marzano, F. Simonelli, and I. Vitiello, "Quasi-dynamic estimation of OD flows from traffic counts: formulation, statistical validation and performance analysis on real data," *Transportation Research Part B: Methodological*, vol. 55, pp. 171–187, 2013.
- [15] H. D. Sherali, R. Sivanandan, and A. G. Hobeika, "A linear programming approach for synthesizing origin-destination trip tables from link traffic volumes," *Transportation Research Part B: Methodological*, vol. 39, pp. 497–518, 1994.
- [16] Y. Nie and D. H. Lee, "An uncoupled method for the equilibrium-based linear path flow estimator for origin-destination trip matrices," *Transportation Research Record*, vol. 1783, pp. 72–79, 2002.
- [17] Y. Nie, H. M. Zhang, and W. W. Recker, "Inferring origin-destination trip matrices with a decoupled GLS path flow estimator," *Transportation Research Part B*, vol. 39, pp. 497–518, 2005.
- [18] S. Tang and H. M. Zhang, "Primal-dual heuristic for path flow estimation in medium to large networks," *Transportation Research Record*, vol. 2333, pp. 91–99, 2013.
- [19] S. Ryu, "Modeling transportation planning applications via path flow estimator," Ph.D. dissertation, Department of Civil and Environmental Engineering, Utah State University, 2015.
- [20] G. Li, "An integrated path flow estimator methodology for multi-modal transportation networks," Ph.D. dissertation, Department of Civil and Environmental Engineering, Hong Kong Polytechnic University, 2022.
- [21] M. Florian and Y. Chen, "A coordinate descent method for the bi-level O-D matrix adjustment problem," *International Transactions in Operational Research* 2, vol. 2, pp. 165–179, 1995.
- [22] Y. Englezou, S. Timotheou, and C. G. Panayiotou, "Path-based origin-destination matrix estimation utilizing macroscopic traffic dynamics," *IEEE Transactions of Intelligent Transportation Systems*, p. 10.1109/ITITS.2024.3370473, 2024.
- [23] X. Zhou, X. Qin, and H. Mahmassani, "Dynamic origin-destination demand estimation with multiday link traffic counts for planning applications," *Transportation Research Record: Journal of the Transportation Research Board*, no. 1831, pp. 30–38, 2003.
- [24] J. Barceló, L. Montero, M. Ballejos, O. Serch, and C. Carmona, "A Kalman filter approach for the estimation of time dependent od matrices exploiting bluetooth traffic data collection," in *91st Transportation Research Board Annual Meeting*. Washington, DC: National Research Council, 2012, pp. 1–16.
- [25] V. Marzano, A. Papola, F. Simonelli, and M. Papageorgiou, "A Kalman Filter for quasi-dynamic OD flow estimation/updating," *IEEE Transactions of Intelligent Transportation Systems*, pp. 1–9, 2018.
- [26] X. Wu, J. Guo, K. Xian, and X. Zhou, "Hierarchical travel demand estimation using multiple data sources: a forward backward propagation algorithmic framework on a layered computational graph," *Transportation Research Part C: Emerging Technologies*, vol. 96, pp. 321–346, 2018.
- [27] W. Ma, X. Pi, and S. Qian, "Estimating multi-class dynamic origin-destination demand through a forward-backward algorithm on computational graphs," *Transportation Research Part C: Emerging Technologies*, vol. 119, p. 102747, 2020.
- [28] J. Ou, J. Lu, J. Xia, C. An, and Z. Lu, "Learn, assign, and search: Real-time estimation of dynamic origin-destination flows using machine learning algorithms," *IEEE Access*, vol. 7, pp. 26 967–26 983, 2019.
- [29] P. Krishnakumari, H. Van Lint, T. Djukic, and O. Cats, "A data driven method for OD matrix estimation," *Transportation Research Part C: Emerging Technologies*, vol. 113, pp. 38–56, 2020.
- [30] N. Zhu, S. Ma, and L. Zheng, "Travel time estimation oriented freeway sensor placement problem considering sensor failure," *Journal of Intelligent Transportation Systems*, vol. 21, pp. 26–40, 2017.
- [31] *Traffic Detector Handbook: Third Edition-Volume II*. Federal Highway Administration, Research, Development, and Technology Turner-Fairbank Highway Research Center, McLean, VA, 2006, no. FHWA-HRT-06-139.

- [32] R. Rajagopal and P. Varaiya, "Health of california's loop detector system," University of California, Berkeley, CA, Tech. Rep., 2007.
- [33] K. Ni, N. Ramanathan, M. Cehade, L. Balzano, S. Nair, L. Zahedi, G. Pottie, M. Hansen, and M. Srivastana, "Sensor network data fault types," *ACM Transactions on Sensor Networks*, vol. 5, 2009.
- [34] A. Ghafouri, A. Laszka, A. Dubey, and X. Koutsoukos, "Optimal detection of faulty traffic sensors used in route planning," *Proceedings of the 2nd International Workshop on Science of Smart City Operations and Platforms Engineering*, pp. 1–6, 2017.
- [35] I. Rapoport and Y. Oshman, "Efficient fault tolerant estimation using the IMM methodology," *IEEE Transactions on Aerospace and Electronic Systems*, vol. 5, pp. 492–508, 2007.
- [36] H. Soken and C. Hajiyev, "Robust adaptive kalman filter for estimation of UAV dynamics in the presence of sensor/actuator faults," *Aerospace Science and Technology*, vol. 28, pp. 376–383, 2013.
- [37] C. G. Claudel, M. Nahoum, and A. M. Bayen, "Minimal error certificates for detection of faulty sensors using convex optimization," *Proceedings of the 47th Annual Allerton Conference on Communication, Control, and Computing (Allerton)*, pp. 1177–1186, 2009.
- [38] J. Corey, Y. Lao, Y. J. Wu, and Y. Wang, "Detection and correction of inductive loop detector sensitivity errors by using Gaussian mixture models," *Transportation Research Record: Journal of the Transportation Research Board*, vol. 2256, pp. 120–129, 2011.
- [39] S. Robinson and J. W. Polak, "Inductive loop detector data cleaning treatments and their effect on performance of urban link travel time models," in *Transportation Research Board 85th Annual Meeting*, no. 06-0989, 2006.
- [40] P. Widhalm, H. Koller, and W. Ponweiser, "Identifying faulty traffic detectors with floating car data," in *IEEE Forum on Integrated and Sustainable Transportation Systems*, 2011, pp. 103–108.
- [41] A. Danczyk, X. Di, and H. X. Liu, "A probabilistic optimization model for allocating freeway sensors," *Transportation Research Part C*, vol. 67, pp. 378–398, 2016.
- [42] M. Salari, L. Kattan, W. H. K. Lam, H. P. Lo, and M. A. Esfeh, "Optimization of traffic sensor location for complete link flow observability in traffic network considering sensor failure," *Transportation Research Part B*, vol. 121, pp. 216–251, 2019.
- [43] N. Alemazkoor, S. Wang, and H. Meidani, "A recursive data-driven model for traffic flow predictions for locations with faulty sensors," *Proceedings of the 21st International Conference on Intelligent Transportation Systems (ITSC)*, pp. 1646–1651, 2018.
- [44] J. Rawlings, "Moving horizon estimation," in *Encyclopedia of Systems and Control*, J. Baillieul and T. Samad, Eds. Springer, 2014, pp. 1–7.
- [45] S. Timotheou, C. G. Panayiotou, and M. Polycarpou, "Moving horizon fault-tolerant traffic state estimation for the cell transmission model," in *IEEE Conference on Decision and Control (CDC)*, Osaka, 2015, pp. 3451–3456.
- [46] S. Aminikhanghahi and D. J. Cook, "A survey of methods for time series change point detection," *Knowledge and Information Systems*, vol. 51, pp. 339–367, 2017.
- [47] C. Alippi, G. Boracchi, D. Carrera, and M. Roveri, "Change detection in multivariate datastreams: Likelihood and detectability loss," *Proceedings of the Twenty-Fifth International Joint Conference on Artificial Intelligence (IJCAI-16)*, pp. 1368–1374, 2016.
- [48] R. P. Adams and D. J. C. MacKay, "Bayesian online changepoint detection," *arXiv preprint arXiv:0710.3742*, 2007.
- [49] Z. Harchaoui, E. Moulines, and F. Bach, "Kernel change-point analysis," in *Advances in Neural Information Processing Systems*, D. Koller, D. Schuurmans, Y. Bengio, and L. Bottou, Eds., vol. 21, 2008.
- [50] E. Keogh and J. Lin, "Clustering of time-series subsequences is meaningless: implications for previous and future research," *Knowledge and Information Systems*, vol. 8, pp. 154–177, 2005.
- [51] D. J. Cook and N. C. Krishnan, *Activity Learning: Discovering, Recognizing, and Predicting Human Behavior from Sensor Data*. Wiley, 2015.
- [52] K. Zhao, M. A. Wulder, T. Hu, R. Bright, Q. Wu, H. Qin, Y. Li, E. Toman, B. Mallick, X. Zhang, and M. Brown, "Detecting change-point, trend, and seasonality in satellite time series data to track abrupt changes and nonlinear dynamics: A Bayesian ensemble algorithm," *Remote Sensing of Environment*, vol. 111181, 2019.
- [53] K. Zhao, "Bayesian changepoint detection and time series decomposition (<https://github.com/zhaoq/rbeast/releases/tag/1.1.2.60>), github. retrieved january 18, 2024."
- [54] D. Park and L. Rilett, "Identifying multiple and reasonable paths in transportation networks. a heuristic approach," *Transportation Research Record*, vol. 1607, pp. 31–37, 1997.
- [55] C. F. Daganzo, "The cell transmission model: A dynamic representation of highway traffic consistent with the hydrodynamic theory," *Transportation Research Part B*, vol. 28, pp. 269–287, 1994.
- [56] —, "The cell transmission model, part II: network traffic," *Transportation Research B*, vol. 29, pp. 79–93, 1995.
- [57] P. Grandinetti, C. Canudas-de Wit, and F. Garin, "Distributed optimal traffic lights design for large-scale urban networks," *IEEE Transactions on Control System Technology*, pp. 1–14, 2018.
- [58] J. Lebacque, "The Godunov scheme and what it means for first order traffic models," in *13th International Symposium of Transportation Traffic Theory*, 1996, pp. 647–677.
- [59] S. V. Ukkusuri, L. Han, and K. Doan, "Dynamic user equilibrium with a path based cell transmission model for general traffic networks," *Transportation Research Part B*, vol. 46, pp. 1657–1684, 2012.
- [60] V. Kekatos and G. B. Giannakis, "From sparse signals to sparse residuals for robust sensing," in *IEEE Transactions on Signal Processing*, vol. 59, 2011, pp. 3355–3368.
- [61] S. Nguyen and C. Dupuis, "An efficient method for computing traffic equilibria in networks with asymmetric transportation costs," *Transportation Science*, vol. 18, pp. 185–202, 1984.
- [62] L. Qing, F. Liao, H. J. P. Timmermans, H. Haijun, and Z. Jing, "Incorporating free-floating car-sharing into an activity-based dynamic user equilibrium model: A demand-side model," *Transportation Research Part B: Methodological*, vol. 107, pp. 102–123, 2018.



Yirolanda Englezou is a postdoctoral Research Associate at the KIOS Research and Innovation Center of Excellence, University of Cyprus since 2018. In 2020 she was awarded a prestigious Marie Skłodowska Curie (MSCA) Widening Fellowship to work on the project "Bayesian Intelligent Transportation Systems (BITS)". Her research focuses on Bayesian inference techniques, machine learning and estimation applications with emphasis on intelligent transportation systems. She received her PhD in Statistics from the University of Southampton in 2018. Her research was within the field of design of experiments, focusing on the development of methods for designing experiments for the calibration of physical and computational models. The work was funded by the UK Engineering and Physical Sciences Research Council and, for a time, the UK Atomic Weapon Establishment. She has also completed a degree in Applied Mathematics and Physical Sciences from the National Technical University of Athens in 2014, where she studied Mathematics, Physics and Computer Science.



Stelios Timotheou (S'04–M'10–SM'17) is an Associate Professor at the Department of Electrical and Computer Engineering and a faculty member at the KIOS Research and Innovation Center of Excellence, of the University of Cyprus. He holds a Dipl.-Ing. in Electrical and Computer Engineering from the National Technical University of Athens, an MSc in Communications and Signal Processing and a PhD in Intelligent Systems and Networks (2010), both from the Department of Electrical and Electronic Engineering of Imperial College London. In previous appointments, he was a Research Associate at KIOS, a Visiting Lecturer at the Department of Electrical and Computer Engineering of the University of Cyprus, and a Postdoctoral Researcher at the Computer Laboratory of the University of Cambridge. His research focuses on monitoring, control and optimization of critical infrastructure systems, with emphasis on intelligent transportation systems and communication systems. Dr. Timotheou is a Senior Editor of the *IEEE Transactions on Intelligent Transportation Systems* and an Associate Editor of the *IEEE Transactions on Intelligent Vehicles*.



mentioned university in 1999. Before joining the University of Cyprus

Christos Panayiotou is a Professor with the Electrical and Computer Engineering (ECE) Department at the University of Cyprus (UCY). He is also the Deputy Director of the KIOS Research and Innovation Center of Excellence for which he is also a founding member. Christos has received a B.Sc. and a Ph.D. degree in Electrical and Computer Engineering from the University of Massachusetts at Amherst, in 1994 and 1999 respectively. He also received an MBA from the Isenberg School of Management, at the afore-

mentioned university in 1999. Before joining the University of Cyprus in 2002, he was a Research Associate at the Center for Information and System Engineering (CISE) at Boston University (1999 - 2002). His research interests include modeling, control, optimization and performance evaluation of discrete event and hybrid systems, intelligent transportation systems, cyber-physical systems, event detection and localization, fault diagnosis, wireless, ad hoc and sensor networks, smart camera networks, resource allocation, and intelligent buildings. He is a Senior Editor for the IEEE Transactions of Intelligent Transportation Systems and an Associate Editor for the Journal of Discrete Event Dynamical Systems, while in the past he served as an Associate Editor for the Conference Editorial Board of the IEEE Control Systems Society, the IEEE Transactions of Control Systems Applications and the European Journal of Control.